Diploma Thesis

Conductive Atomic Force Microscopy Investigations of Organic Thin Films

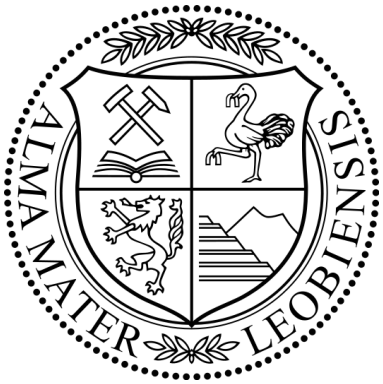

Andreas Pavitschitz

Performed at the

Institute of Physics

University of Leoben

under the supervision of

Prof. Dr. Christian Teichert

Dr. Markus Kratzer

refereed by

Prof. Dr. Christian Teichert

Leoben, December 2010

EIDESSTATTLICHE ERKLÄRUNG

Ich erkläre an Eides statt, dass ich diese Arbeit selbstständig verfasst, andere als die angegebenen Quellen und Hilfsmittel nicht benutzt und mich auch sonst keiner unerlaubten Hilfsmittel bedient habe.

AFFIDAVIT

I declare in lieu of oath, that I wrote this thesis and performed the associated research by myself, using only literature cited in this volume.

_____ _____

Datum Unterschrift

dedicated to Marlies and my parents

Abstract

Organic thin films are of increasing importance as electronic material for various applications like, for example, organic light emitting diodes (OLEDs) and dielectric thin films in organic field effect transistors (OFETs). The surface morphology and the local electric conductivity of these films are of particular importance for their functionality.

In this thesis, the surface morphology and electrical conductivity of dielectric parylene layers as well as photoreactive polyaniline thin films were investigated. For this purpose, conductive atomic-force microscopy (C-AFM) was applied. C-AFM allows a simultaneous determination of the surface morphology and the electrical conductivity on the nanometer-scale.

Parylene films on Ag/glass showed good insulating behavior, but poor mechanical resistance. The surface of parylene on Ag/glass is uneven with an RMS roughness of 3.5 nm. The voltage dependence of the tunneling current through the films, could not be explained by Fowler-Nordheim behavior.

The polyaniline thin films were illuminated by UV-light through masks which were patterned in the micrometer range. The conductivity of the photosensitive polyaniline thin films increased upon ultraviolet (UV) light exposure to a value just above the detection level of the used C-AFM. A significant increase in conductivity of the UV illuminated areas could be achieved via protonation in HCl vapor.

Kurzfassung

Dünne organische Schichten gewinnen im Bereich der Elektronik einen immer breiteren Raum für Anwendungen. Bereits realisierte Anwendungen sind beispielsweise organische Leuchtdioden (OLEDs) sowie dielektrische Schichten in organischen Feld-Effekt-Transistoren. Speziell die Oberflächenbeschaffenheit und die lokalen elektrischen Eigenschaften der organischen Dünnschichten sind von Bedeutung für ihre Funktionalität.

In dieser Arbeit wurden dielektrische Parylenfilme sowie photoreaktive Polyanilinfilme bezüglich ihrer Oberflächenmorphologie und elektrischen Leitfähigkeit untersucht. Dabei wurde Leitfähigkeits–Rasterkraftmikroskopie (Conductive Atomic-Force Microscopy, C-AFM) eingesetzt, welche eine gleichzeitige Messung der elektrischen Leitfähigkeit und der Oberflächenbeschaffenheit auf der Nanometerskala ermöglicht.

Die Parylene–Filme auf Ag/Glas zeigten hohes Isolationsvermögen aber geringe mechanische Festigkeit. Die Oberfläche ist uneben mit einer RMS Rauigkeit von 3.5 nm. In den Strom–Spannungs Kurven konnte Tunnelverhalten gesehen werden, welches aber nicht schlüssig durch die Fowler–Nordheim Theorie zu erklären ist.

Die UV-reaktiven Polyanilinfilme wurden durch – im Mikrometerbereich strukturierte - Masken belichtet, wodurch es in den belichteten Bereichen zu einem mit dem verwendeten C-AFM gerade noch detektierbaren Leitfähigkeitsunterschied führt. Durch Protonierung in Salzsäuredampf konnte die Leitfähigkeit der belichteten Bereiche signifikant gesteigert werden.

Contents

1 Introduction

Organic materials are already widely used as insulators in electronic devices and electric components. More recent applications are organic semiconductors and organic conductive materials. Organic semiconductors are one of the most promising materials of the 21st century. In 2000, the Nobel prize for chemistry was awarded to Alan J. Heeger, Alan McDiarmid, and Hideki Shirakawa for the discovery and the development of conductive polymers. Organic semiconductors are the basis for applications like large-area flexible light sources and displays, organic solar cells, and low cost integrated circuits. Organic conductive materials can be used as electric connections or transparent electrodes. Advantages of organic electronics compared to traditional inorganic semiconductors are the lower production costs, the wide range of characteristics and the possibility to form flexible films. Drawbacks of organic electronics are their mechanical and thermal instability and the decomposition of the polymer under UV radiation. To improve organic electronic devices, fabricated by thin film techniques, knowledge about the surface morphology and the electronic properties is of fundamental importance. The production of electronic devices with small scale structures requires a technology to influence the conduction behavior of organic thin films on the sub - µm scale. Especially UV sensitive polymers promise to allow a patterning and a functionalization of films in organic electronics with fast and reliable technologies on well defined areas. The performance of thin film electronic devices is strongly depending on the surface morphology of the organic thin film and its electric properties.

Scanning probe microscopy, like atomic force microscopy (AFM) (see chapter 2.1), allows to map the surface morphology with nm scale lateral resolution. Conductive atomic force microscopy (C-AFM) (see chapter 2.3) is a variation of AFM. In C – AFM, it is possible to map the local film conductivity on the nanometer scale simultaneously to the surface morphology. The details of carrier characteristics can be explored with local I-V curves.

In this study, conductive atomic force microscopy (C-AFM) was used to investigate dielectric and semiconducting polymers on different substrates. Parylene was investigated as a dielectric material with special focus on surface coverage and film homogeneity to

find a lower limit of film thickness to use parylene as an insulator. In the course of finding a polymer which is changing its conductivity after UV illumination, samples of a poly(diphenyl bicyclo[2.2.1]hept-5-ene-2,3-dicarboxylate) (PPNB)/ Poly (N-vinylcarbazole) (PVK) polymer blend, Polyformyl-ortho-toluidine (PFOT) and a modified polyaniline (PANI) were investigated. The UV sensitive polymers were illuminated through masks with periodic transparent and non-transparent areas in µm size. [1-5]

2 Fundamentals

2.1 Atomic Force Microscopy (AFM) – General

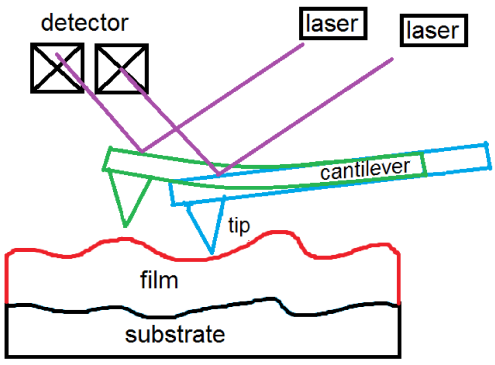

Fig. 1: Principle of surface mapping by AFM

In atomic force microscopy (AFM), a sharp tip on a flexible cantilever is scanned across the surface by means of a piezoelectric scanner. Fig. 1 shows the working principle of an AFM in contact mode surface mapping. The scanner is moving the cantilever with the tip over the sample, or the sample is moved under the tip. Repulsive forces between the tip and the sample cause a bending of the cantilever. When the lateral height of the sample changes, the bending changes as well. This is detected via a laser beam which is reflected from the backside of the cantilever onto a photo-diode. In constant height mode the cantilever is scanning over the surface in a constant height (constant piezo voltage) and the morphology is mapped with the photo-diode signal. In constant force mode the tip is pressed with a constant force (constant bending of the cantilever) onto the sample. The force can be calculated using the spring-constant of the cantilever and the photo-diode signal. To keep the force constant, a feedback loop regulates the bias of the piezoscanner by maintaining the position of the laser beam on the photo-diode (and therefore the force) constant. The surface morphology is determined from the voltage that is applied to the piezoscanner to enable the necessary height change. [4]

2.2 Friction Force Microscopy (FFM)

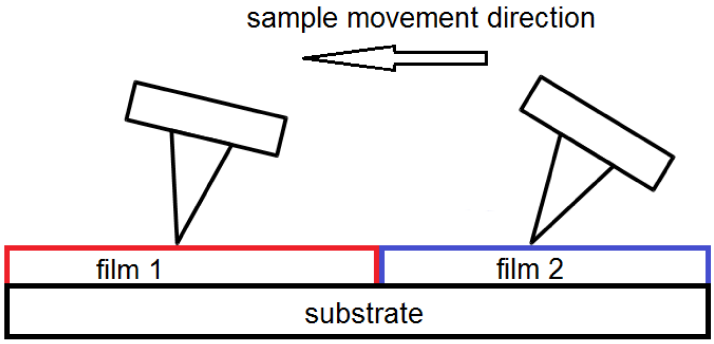

Fig. 2: Principle of Friction Force Microscopy (FFM)

Friction force microscopy (FFM) is an alternative operation mode of an AFM in contact mode. In friction force microscopy, the cantilever is moved perpendicularly to its length axis over the surface as can be seen in Fig. 2. The morphology is causes a bending of the cantilever, and the friction between tip and sample results in a torsion of the cantilever. This torsion moves the laser beam in lateral direction on the photo-diode. Different surface phases may differ in their friction coefficient, and this difference is mapped in FFM. [5]

2.3 Conductive Atomic Force Microscopy (C – AFM)

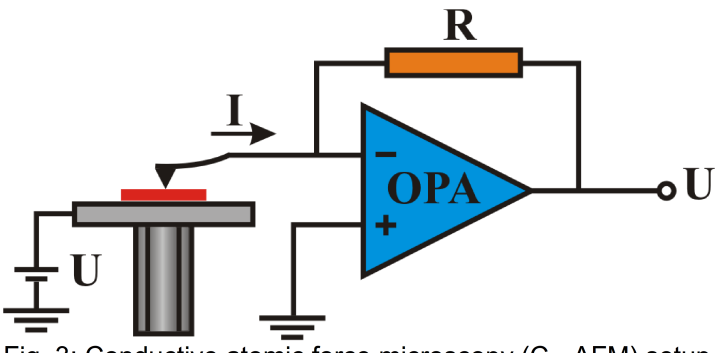

Fig. 3: Conductive atomic force microscopy (C - AFM) setup

In C–AFM conductive probes are used, and the measurements are performed in contact mode. In Fig. 3 the principle of C – AFM is shown. In C – AFM, the sample is biased. This

results in a current flow through the conductive tip. The current is transformed by a current to voltage amplifier into an amplified signal in the proximity of the probe. Keeping the applied voltage constant during measurement allows a simultaneous and independent mapping of the morphology and the local conductivity of the sample surface on the nanometer-scale. The resulting 2D morphology maps are called height images, and 2D current maps are called current images at a certain voltage. The details of carrier characteristics of a single spot can be explored by keeping the tip in a certain position and by applying a voltage ramp to measure a local current-voltage (I - V) curve. For inorganic dielectrics like SiO_2, ZrO_2 and HfO_2 an investigation in ultra high vacuum is necessary to avoid additional film growth, caused by atmospheric oxygen and water, during measurement [4]. For the measurements of organic films it is assumed here that operating under ambient conditions will not influence the investigated film.

2.4 C – AFM Investigations of Organic Thin Films

Due to of the weaker mechanical properties of organic semiconductors compared to inorganic semiconductors [1], one has to pay more attention to the used tip and cantilever and the applied force to avoid a destruction of the film surface. In current mapping, also the special electric properties of organic semiconductors have to be considered. Especially the space charge limited current (SCLC) [2] and the dependence of the carrier mobility on the applied electric field influences the measurement. The carrier mobilities determined from I-V curves performed with a C – AFM can differ by orders of magnitude to the carrier mobilities measured in planar SCLC or time - of – flight measurements. (see also chapter 2.6.2). Carrier injection with a sharp tip causes a larger SCLC than planar electrodes. This effect also reduces the resolution of C – AFM current mapping. [2,3]

2.5 Fowler – Nordheim Tunneling

By Fowler – Nordheim tunneling we understand the tunneling of electrons through a metal – insulator – semiconductor structure. When applying a voltage between the metal and the semiconductor on such a structure, the valence band and the conduction band of the insulator are bent. If the bending is strong enough electrons can overcome the band gap

and a current flows. I–V curves of such a structure show a typical breakdown voltage, where the resistance becomes finite. By applying the Fowler – Nordheim (FN) equation on measured I–V curves, one can estimate the thickness, the work function and the effective electron mass of the dielectric film. In Fig. 4 an exemplary FN – Curve is shown. [6-9]

The FN – tunneling current can be described by the following equations [7]:

$$I = A_{eff} \frac{e^3}{8\pi\phi h} \frac{V^2}{d^2} \, \mathrm{e}^{\frac{-d}{V}\frac{8\pi\phi^{3/2}}{3eh}\sqrt{2m_{eff}}} \tag{1}$$

$$A_{eff} = \pi r_c^2 \tag{2}$$

$$r_c^3 = \frac{3}{4}(\kappa_1 + \kappa_2) F_{fts} R_{tip} \tag{3}$$

$$\kappa_i = \frac{1-\nu_i}{E_i} \tag{4}$$

The tunneling current density depends on the applied bias, the tunneling barrier height and the film thickness.

The resulting tunneling current is the product of the tunneling current density and the effective tunneling area. An exemplary I - V curve can be seen in Fig. 4. The effective tunneling area for a current flow through a sharp, conductive tip and a planar insulator depends on the tip radius, the applied force between tip and sample and the elastic constants of both.

The parameters needed in the FN–curver are:

A_{eff}	effective tunneling area
I	tunneling current
e	positive electron charge
m_{eff}	effective electron mass in the insulator

ϕ	barrier height
V	bias across the surface
d	film thickness
h	Planck constant
r_c	radius of contact area
E_i,	Young's moduli of the tip and sample
v_i	Poisson's ratio of the tip and sample

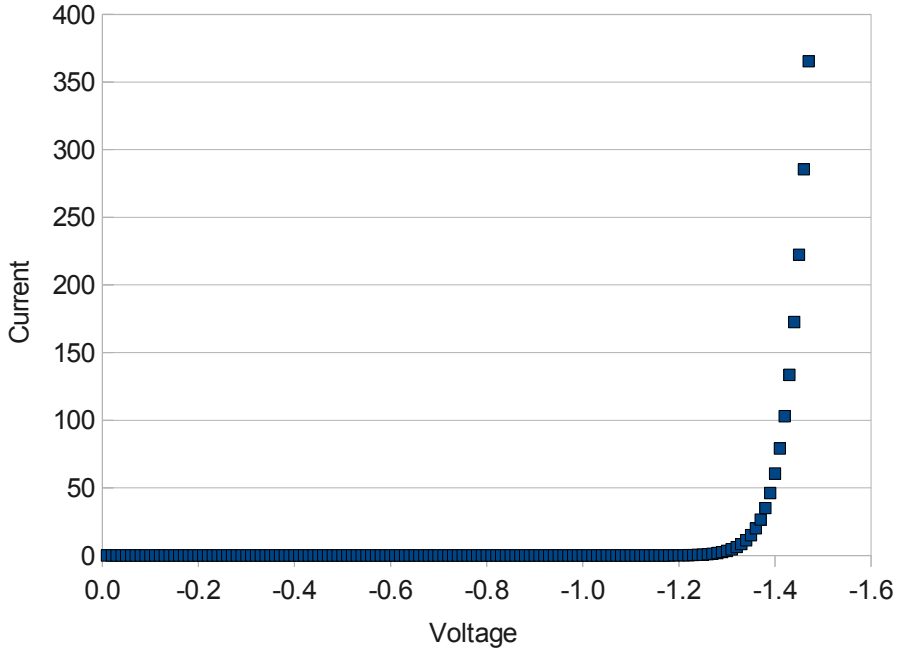

Fig. 4: Exemplary FN - Curve

Pseudo Break Down Voltage (PBDV)

In order to get statistical information about the distribution of the conductivity or the average fraction of conductive and non-conductive areas a so-called pseudo breakdown voltage is used. A certain current is defined, and the voltage at this current is the PBDV. From a number of I-V curves the PBDV can be recorded and be plotted in a histogram. [6]

2.6 Physics of Organic Dielectrics and Semiconductors

2.6.1 Organic Dielectrics

The majority of organic materials in electrics and electronics are used as electric insulators. Due to their flexibility, chemical and environmental resistance and low cost, polymers are used for applications like wire coatings, structural components and protective coatings for printed circuits. In organic electronics, dielectric materials are applied as gate dielectrics and electric insulating material. [1, 10-13]

2.6.2 Organic Semiconductors

Organic semiconductors are in many ways different from inorganic semiconductors. Inorganic semiconductors like Si or GaAs form highly ordered crystals, where the single atoms are arranged in perfect periodic order. In contrast, organic semiconductors consist of rather large hydro carbon based molecules, which may contain also other nonmetallic elements like nitrogen, sulfur and chlorine or even metals. The molecules can be stoichiometric or statistical in molecular weight. The atoms within the molecules are also covalently bonded. The inter-molecular bonds originate from van der Waals forces which leads to the formation of organic crystals or amorphous organic solids. The weak van der Waals forces determine the specific mechanical and thermodynamic properties of organic semiconductors, like reduced hardness and melting point. The electric properties are crucially determined by the weak electronic delocalization among neighboring molecules. Due to the weak electronic delocalization the optical absorption and luminescence spectra of organic molecular solids are similar to those of the gas phase or solutions. This can be seen in Fig. 5, where Δ1 and Δ2 indicate the shift from gas phase to the solvent and further-on to the solid state. Disordered organic solids show a spectral broadening. [1]

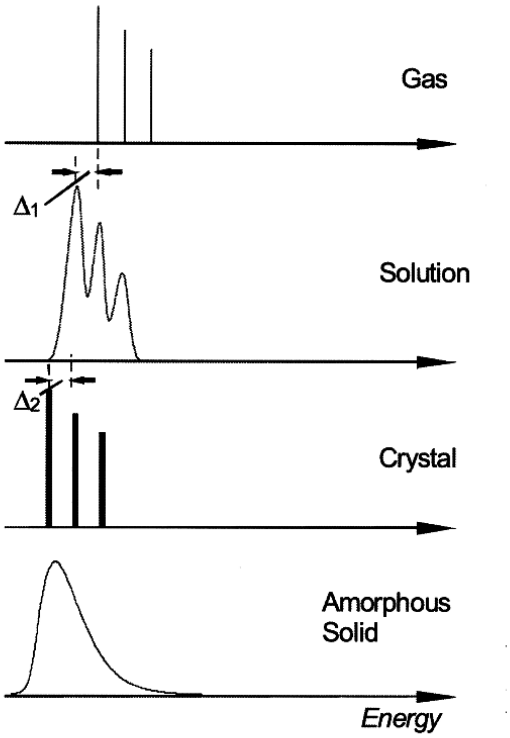

Fig. 5: Schematical presentation of optical spectra of organic molecules in different surroundings. [1]

Charge Carrier Transport

The transport of electrons or holes in an organic solid requires ionic molecular states. An electron is removed from a neutral molecule M and forms a radical cation M^+ and a negatively charged anion M^-. In case of polymers, the charged states are usually called positive or negative polarons. In Fig. 6 the energy levels for an isolated molecule, a molecular crystal and an amorphous solid are compared. The Gaussian density of states for an organic solid is caused by the different molecular environments. In extreme cases of organic semiconductors two extrema of transport mechanisms are possible. There is band transport, similar to anorganic semiconductor crystals, for pure highly ordered molecular crystals at moderate temperatures and so called hopping transport for amorphous solids. The mobility for band transport at room temperature is in the range of 1 to 10 cm^2/Vs and about 10^{-3} cm^2/Vs for hopping transport. For organic semiconductors the mobility depends on the applied electric field and the temperature. [1, 11, 12]

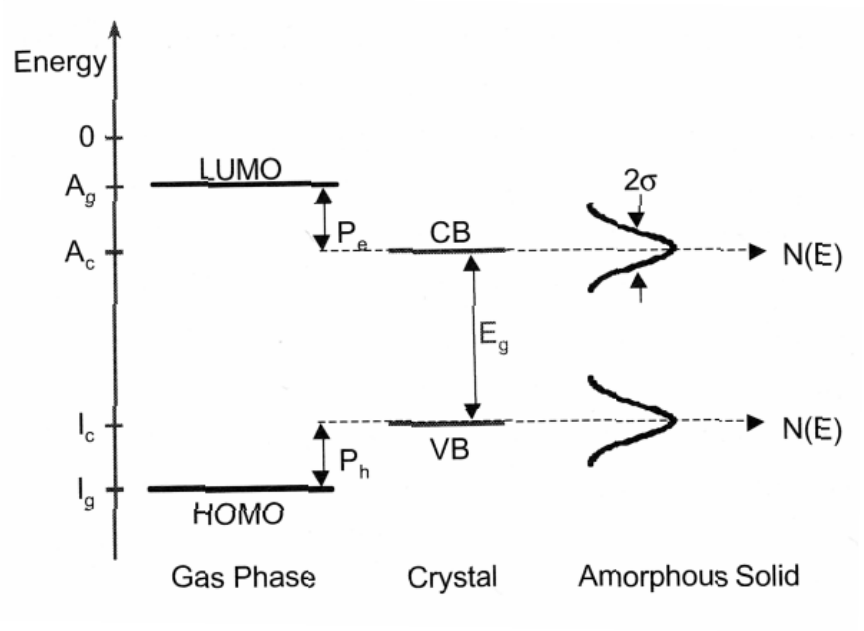

Fig. 6: Energy levels of an isolated molecule, a molecular crystal and an amorphous solid [1]

2.7 Investigated Organic Thin Films

2.7.1 Parylene

Parylene is a polymer which is based on the structure presented in Fig. 7 a. For this investigation, so called parylene C was used. In parylene C, one of the hydrogen atoms in the aromatic ring is substituted by a chlorine atom. Parylene is a chemically inert, hydrophobic, optically transparent, thermodynamically stable, bio-compatible, and bio-stable coating material. The electric properties are a low dielectric permittivity and a high electric strength.

a) b)

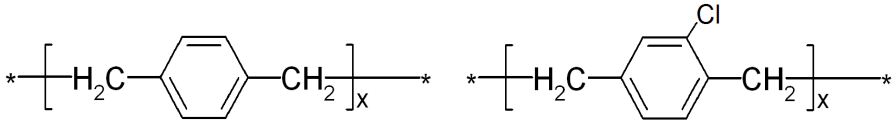

Fig. 7: Chemical formula of a) Parylene and b) Parylene C

Fig. 8 shows the principle of parylene coating from Comelec company. In the heating area the solid dimer sublimates into a dimeric gas at about 100°C. Furtheron the dimer is cracked to a monomer in a high temperature zone at about 700°C. In the deposition chamber the monomer is polymerizes into a thin film at room temperature and a at pressure of 10^{-2} mbar. The chemical vapor deposition (CVD) process makes it possible to deposit parylene in thin films without pinholes with high homogeneity on edges and sharp tips and also in deep trenches. Deposition at room temperature allows to coat nearly every material. Usual applications use film thicknesses from 0.1 µm to 50 µm. It is possible to coat most of the materials like metals, ceramics and polymers. These properties make parylene an already widely used material in various applications. For example as protective and insulating coating for printed boards or as bio-accepted layer on medical devices. [10, 13]

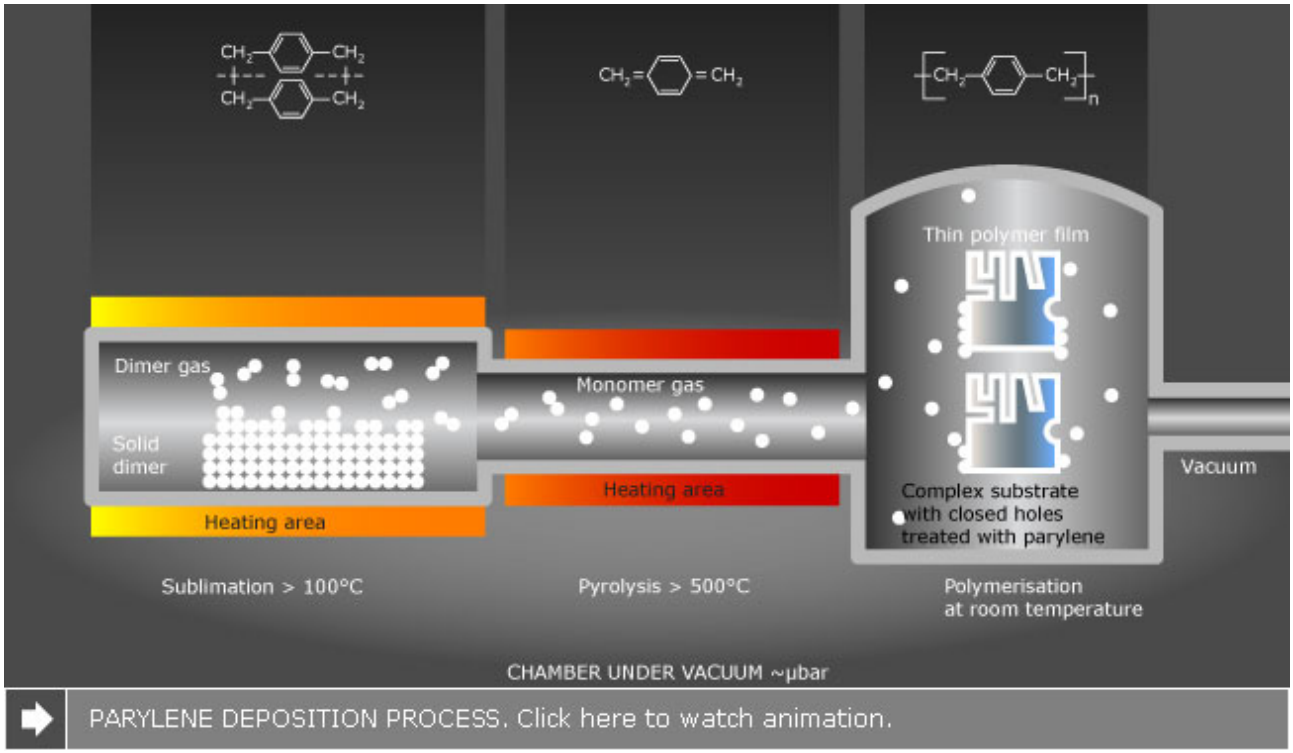

Fig. 8: schematic Parylene deposition process from Comelec [13]

2.7.2 Polyaniline, Poly-N-formylaniline (PANI)

Polyaniline (PANI) is a conductive polymer, having 6 – edged carbon rings linked with nitrogen. The electronic properties of polyaniline depend on the number of electrons and protons. There are insulating, semiconducting and metallic conductive kinds of PANI possible. Exposing PANI to Bronsted - acids is causes a diffusion of H^+ ions into the polymer. This is called proton doping or protonation. The conductivity of PANI can be improved over several orders of magnitude by proton doping.

Upon UV irradiation the poly-N-formylaniline undergoes a photo-decarbonylation reaction leading to polyaniline (Fig. 9). UV-illumination through a mask and protonation allows to pattern films of PANI with conductive and nonconductive areas. [14,15]

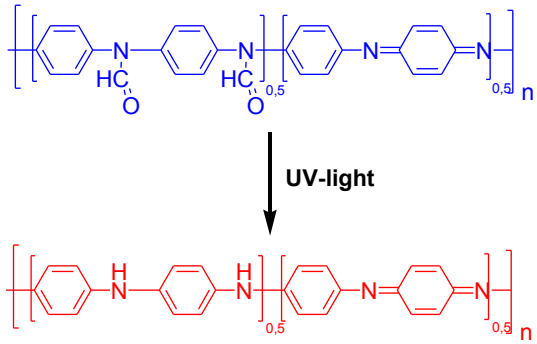

Fig. 9: Polyaniline transformation

2.7.3 Poly-N-formyl-ortho-toluidine (PFOT)

PFOT is the methyl substituted form of Poly-N-formylaniline with a structure shown in Fig. 10. UV illumination of PFOT is causing a chemical change similar to PANI described in 2.7.2. Advantageous of PFOT compared to PANI is the better solubility in organic solvents. [16]

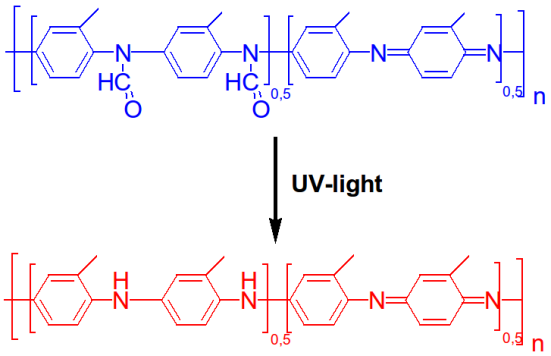

Fig. 10: PFOT transformation

2.7.4 Poly(endo,exo-bicyclo[2.2.1]hept-5-ene-2,3-dicarboxylic acid, diphenyl ester) (PPNB) / Polyvinylcarbazole (PVK) PPNB/PVK

Poly(endo,exo-bicyclo[2.2.1]hept-5-ene-2,3-dicarboxylic acid, diphenyl ester) (PPNB)

The structure of PPNB before and after UV-illumination is shown in Fig. 11. The UV-induced reaction of aryl esters to the corresponding para and ortho ketones is called photo Fries rearrangement. This chemical reaction changes the refractive index and the surface polarity of the polymer.[15]

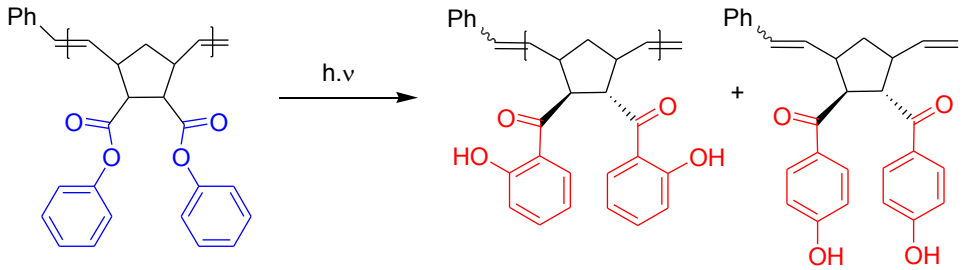

Poly-1

Fig. 11: PPNB transformation

Polyvinylcarbazole (PVK)

PVK is a conductive polymer with a structure shown in Fig. 12. PVK is used as a hole transport layer for organic electroluminescent devices. It is chemically not influenced by UV-illumination, but a photoconductive behavior is known. [17,18]

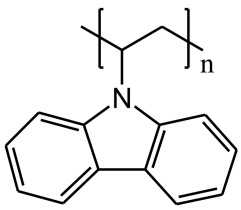

Fig. 12: PVK

3 Experimental

3.1 Sample Preparation

3.1.1 Polymerization

All Parylene films were grown by polymerization of C- parylene on Ag/glass and provided by G. Schwabegger and the group of H. Sitter, JKU Linz.

3.1.2 Spin Coating

Spin coating is a method to cover flat surfaces with a well defined and homogeneous liquid film. To deposit a solid polymer, the polymer has first to be brought into solution in an organic solvent. N,N-Dimethylformamid was used as a solvent for the spin coated PANI films in this investigation. The substrate is placed on a disk, and a vacuum system sucks the substrate onto the disk to keep it in position. The disk is brought into spinning, and a droplet of the liquid drops on the spinning substrate and is spread over the surface due to centrifugal forces. After coating, the sample can be heated to evaporate the remaining solvent. The resulting film thickness is influenced by the surface morphology of the sample, surface energy between liquid and substrate, the viscosity of the liquid and the rotation speed of the disk. [19]

3.1.3 Mask Illumination

The UV-sensitve samples investigated in this thesis were illuminated through the proximity mask shown in Fig. 13. The mask has several features like suns and lines on it with sizes in the range of several mm down to µm. The features were written by an electron beam writer. In Fig. 13, the mask is placed on an Au/glass substrate. The mask is, like common masks in semiconductor industry, a glass plate with a chromium layer. [19]

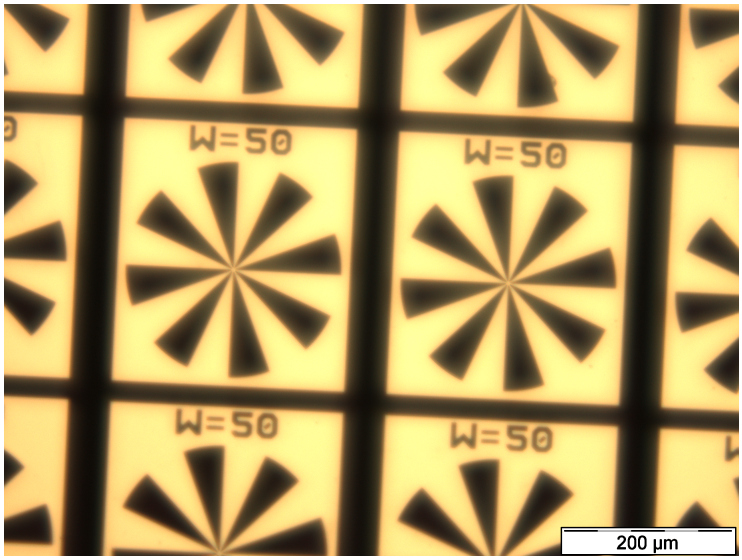

Fig. 13: Contact mask

3.2 Atomic Force Microscope (AFM)

All investigations were performed on a Digital Instruments multi mode AFM under ambient conditions. The AFM was operated in constant force mode. For C-AFM measurement a home built amplifier for C–AFM was employed [6]. The noise level of the resulting setup for C–AFM is about 60 fA.

3.3 C - AFM Probes

For C–AFM, conductive tips and cantilevers are required. The tip should be sharp for a high lateral resolution. However a small tip radius also decreases the contact area for electric charge transport. The AFM investigation of soft matter, like polymer films, requires a cantilever with a low force constant to reduce the damage caused by the lateral force between tip and sample. However, a certain force is required to ensure the electric contact for the C–AFM measurement. During investigation, various cantilevers were tested, but only two types worked. They are described below.

3.3.1 TiN Coated Silicon Probes

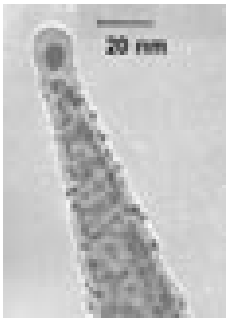

Fig. 14: TiN CSG 01 cantilever from NT-MDT

The TiN coated single crystal n-doped Si cantilevers from NT-MDT have a typical force constant of 0.03 N/m and a tip radius of 35 nm [20]. The very long and soft cantilevers proved a good imaging quality in topography and current mapping. The 25 nm thick TiN – coating exhibits metallic conductivity and has a high wear resistance on the investigated polymers and only a small tendency to pick up particles from the surface. The cantilevers worked very well on PPNB/PVK, PFOT, and PANI but they did not work at all on parylene films or pure silicon. It was also possible to perform friction force measurements with these cantilevers.

3.3.2 Diamond Coated Silicon Probes

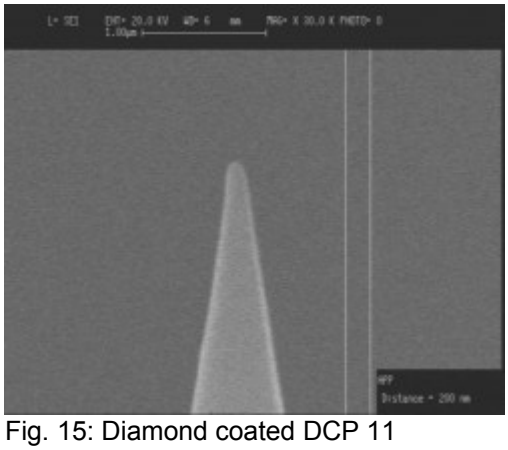

Fig. 15: Diamond coated DCP 11 cantilever from NT-MDT

The single crystal boron doped Si cantilevers with nitrogen doped diamond coating from NT-MDT have a typical force constant of 11.5 N/m and a tip radius of 70 nm. The 70 nm

thick diamond coating has a resistivity of 0.5 – 1 Ωcm and a high wear resistance. [20] The stiff and rough cantilevers scratch the polymer films and lose their quality in current mapping by picking up non-conductive particles from the surface. Nevertheless, the diamond coated cantilevers were the only ones which allowed investigating the parylene films.

3.4 AFM Analysis Software

For data acquisition, the built-in Digital Instruments software was used. For all data processing, analyzing and image generation the free software Gwyddion 2.19 was used. Gwyddion is a free SPM data visualization and analysis tool for various SPM systems and computer platforms [21].

3.4.1 RMS Roughness

The Root Mean Square Roughness is: *"The average of the measured height deviations taken within the evaluation length and measured from the mean line."* [21]

$$\sigma = \sqrt{\frac{1}{MN}\sum_{j=1}^{N}\sum_{i=1}^{M}(z(x_i, y_j) - \langle z \rangle)^2} \qquad (6)$$

M	Sum of points in x direction
N	Sum of points in x direction
z	height in point (x_i, y_j)
x_i	x coordinate of point
y_j	y coordinate of point

The σ value depends on the analyzed image size. Here areas between 10µm^2 and 50µm^2, depending on the feature size, were measured.

3.4.2 Calculation of the Friction Force Images

The lateral deflection is influenced by the friction between the tip and the surface and the surface morphology. To get a real friction force image one has to eliminate the morphology influence from the lateral signal. The morphology influence is the same in trace and retrace direction, while the friction information is symmetrical. Subtracting (for example) the lateral deflection value for every single point in trace direction from retrace direction eliminates the morphology value and results in a real friction force image. This can easily be done by the Gwyddion software.

$$F_{FR}(x,y) = LD_t(x,y) - LD_r(x,y) \quad (7)$$

$F_{FR}(x,y)$ friction force

$LD_t(x,y)$ lateral deflection trace

$LD_r(x,y)$ lateral deflection retrace

4 Results

4.1 Parylene Dielectric Films

The parylene samples were provided by Günther Schwabegger from the group of Prof. Helmut Sitter, JKU Linz. Different film thicknesses on different substrates were investigated.

4.1.1 28 nm Parylene Films on Ag

Fig. 17 shows representative C – AFM results from a sample with 28 nm parylene on Ag / glass. The height image [Fig. 17a] shows an uneven surface with heights up to 40 nm, diameters up to 300 nm and an RMS roughness of 3.5 nm. In the current image [Fig. 17b], conductive and non-conductive areas can clearly be distinguished. The conductive areas are round or elongated with a lateral size up to 65 nm. The combination of height- and current image [see Fig. 17c] shows higher conductivity mainly in protruding areas. There are two options to explain this behavior, which are illustrated in Fig. 16. As can be seen in the left part of the illustration, a higher film thickness in the lowered areas of the rough substrate would exhibit a higher resistivity. Another possibility is shown in the right part, meaning that the AFM tip is scratching the film on protruded areas.

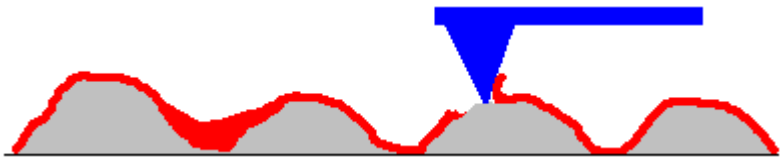

Fig. 16: Possible explanations for the conductive areas observed on parylene on Ag/glass.

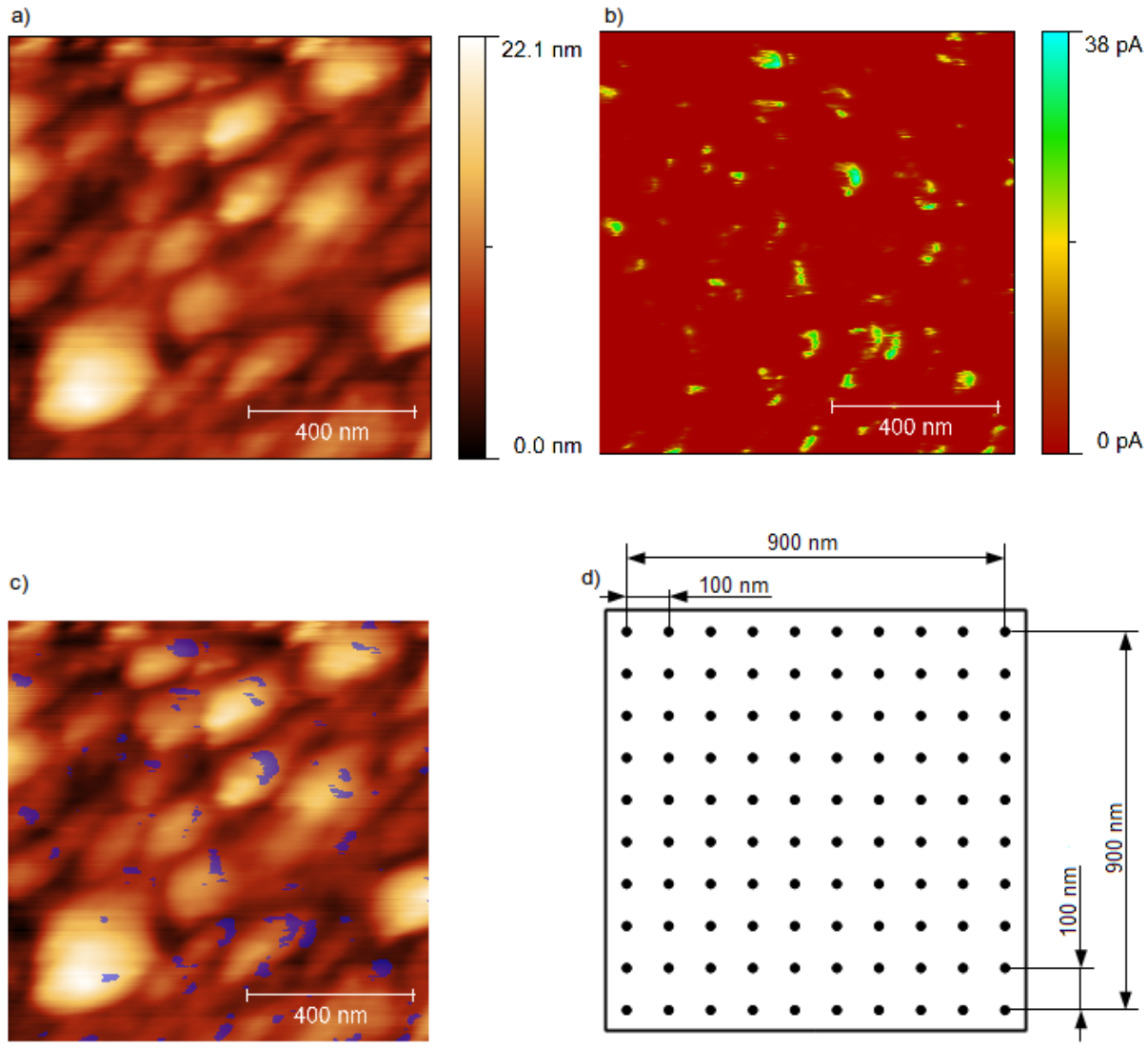

Fig. 17: 28 nm Parylene on Ag/glass; a) height image, b) current image @ - 0.02 V, c) height image with current mask, d) raster of I – V curve measurement points

4.1.2 I-V Curves on 28 nm Parylene on Ag/glass

The histogram plot in Fig. 18 a) was performed by measuring 100 surface points on a 900x900 nm grid with a pitch of 100 nm as shown in Fig. 17 d). At least 3 curves were recorded on each point. The pseudo breakdown voltage was defined at a level of 50 pA. The average voltage @ 50 pA for every spot was recorded and sorted in groups. The sum for every group was plotted over the voltage to obtain the histogram. For Fig. 18 b), the

spots showing tunneling behavior or ohmic behavior were counted. Most of the measured points show a current already at very low voltages and thus the surface appears to be only about 20% covered with parylene.

The I – V curves of the conductive areas in Fig. 19 a) are almost perfectly linear and do not change during the measurement. This implies ohmic behavior. Thus, one can conclude that there is no dielectric material between tip and sample. The effective tunneling area was calculated roughly as 15 nm² for the contact between silver and a diamond coated tip with a curvature radius of 35 nm.

Tunneling behavior can be seen in the I – V curves recorded on higher conductive areas [Fig. 19 a)], and the presence of a dielectric material on the sample surface can be concluded. The contact between the parylene and the diamond coated tip exhibits unstable behavior with time. A lowering of the tunneling barrier during series of measurements at the same point is observed. This could be explained on the one hand by the viscoelasticity of parylene causing a decrease in film thickness. On the other hand, this behavior might result from changes in the electric properties of the parylene – tip interface or damage of the film due to chemical degradation or electric charge flow.

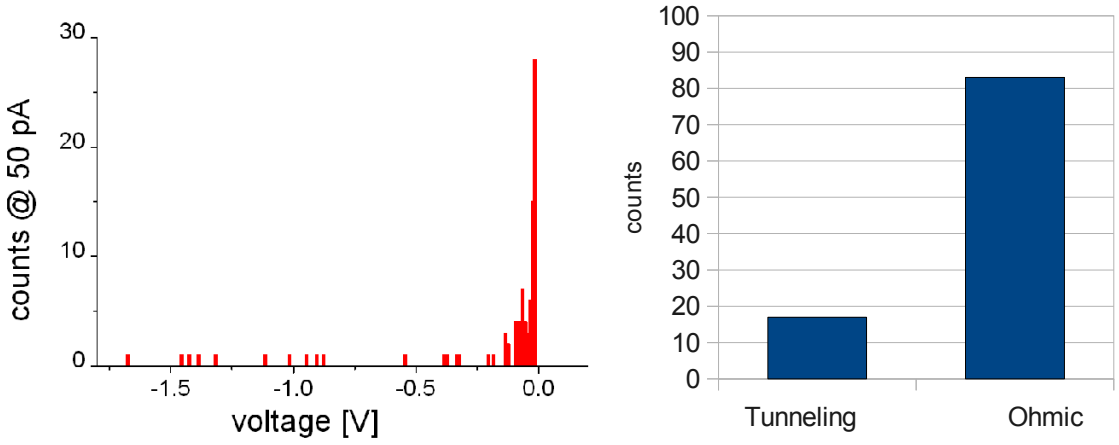

a) b)

Fig. 18: Histogram of pseudo breakdown voltages measured on parylene on Ag/glass, calculated from 100 I-V curves, a) histogram b) number of tunneling and ohmic spots

a)

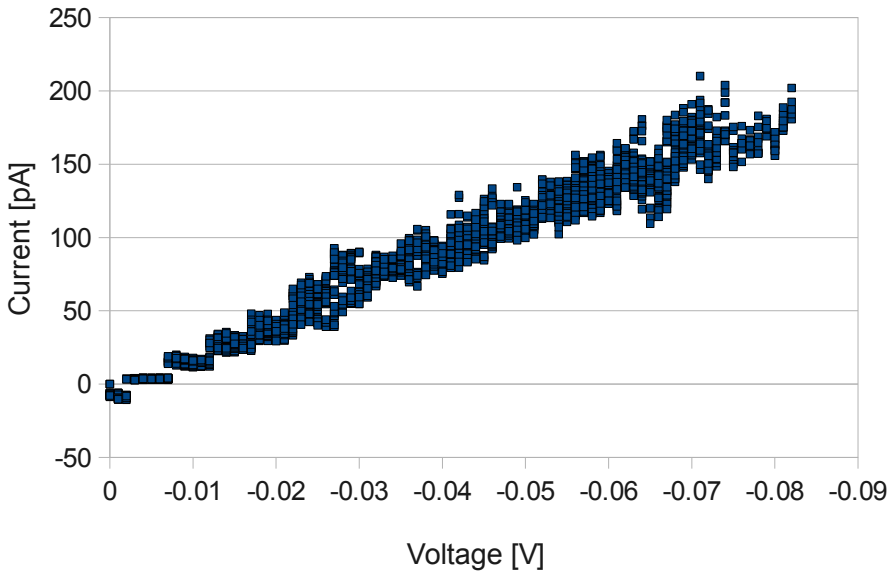

b)

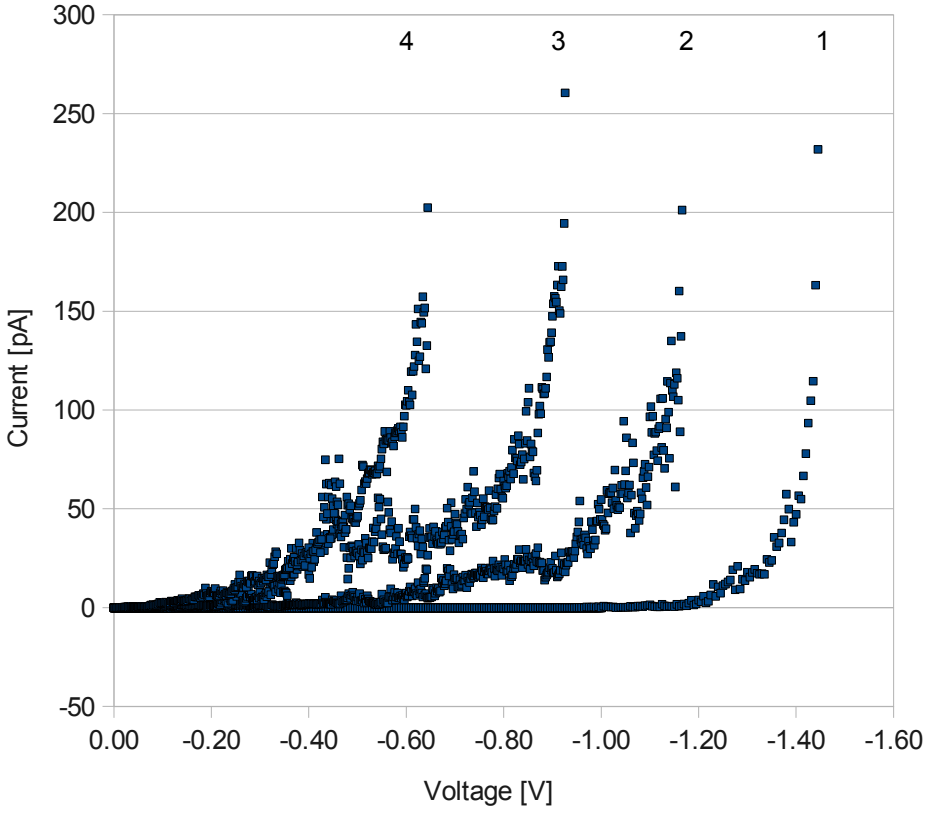

Fig. 19: I - V curves of 28 nm Parylene, a) on conductive area, b) on non conductive area

4.1.3 Fowler-Nordheim Analysis

In Fig. 20, the measured curve is fitted by a Fowler Nordheim curve. Formula (8) was used for the fit with 10^{14} A/V^2 as constant parameter K_1 for the squared term and 50 V as K_2 in the exponent. The only variable parameter is the voltage V.

$$I = K_1 V^2 \, e^{\frac{-K_2}{V}} \tag{8}$$

The fit meets the measured curve very well, but unfortunately it was not possible to fit the measured curve with physically realistic parameters for the work function, the effective electron mass, the contact area and the film thickness. This means Fowler - Nordheim tunneling behavior is not proven.

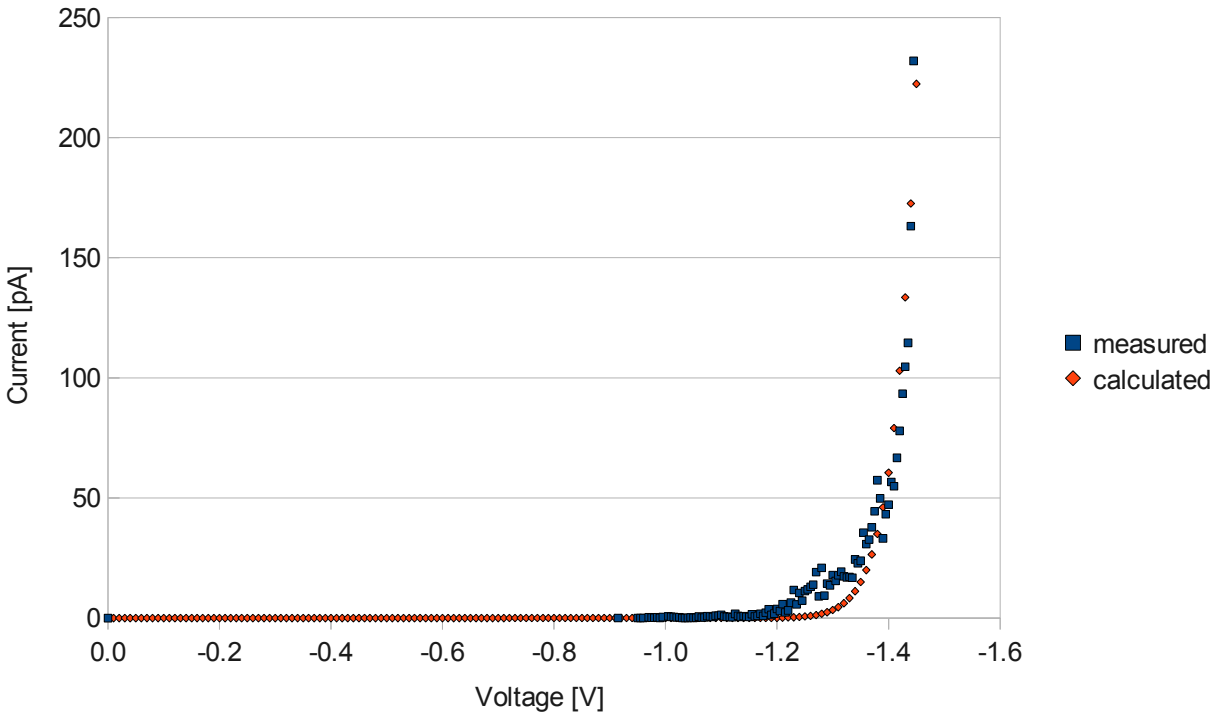

Fig. 20: Fowler – Nordheim fit to the measured data

4.2 PPNB / PVK

The Poly(endo,exo-bicyclo[2.2.1]hept-5-ene-2,3-dicarboxylic acid, diphenyl ester) / Polyvinylcarbazole (PPNB/PVK) polymer blend was spin coated on silicon wafers and afterwards illuminated through a 15 µm lines and spaces mask by the group of Thomas Griesser at the Institute of Chemistry of Polymeric Materials, University of Leoben. Fig. 21 represents topography (a), C – AFM (b) and FFM (c) of the same 50 µm x 50 µm surface area. The AFM measurements were performed immediately after the sample preparation, and the sample was always protected from ambient UV light. In Fig. 21a) a heterogeneous surface morphology is observed. The RMS roughness is 21.8 nm for 50 µm x 50 µm scan size. Two morphological features are observed: round structures with a diameter of about 460 nm and elongated structures with a width of about 540 nm and an average length of 2900 nm embedded in a matrix. Also the current and the friction images show these structures. The illumination with UV radiation through a 15 µm mask does not change the morphology or the electric behavior. However, a clear effect on the matrix material in friction force contrast can be seen.

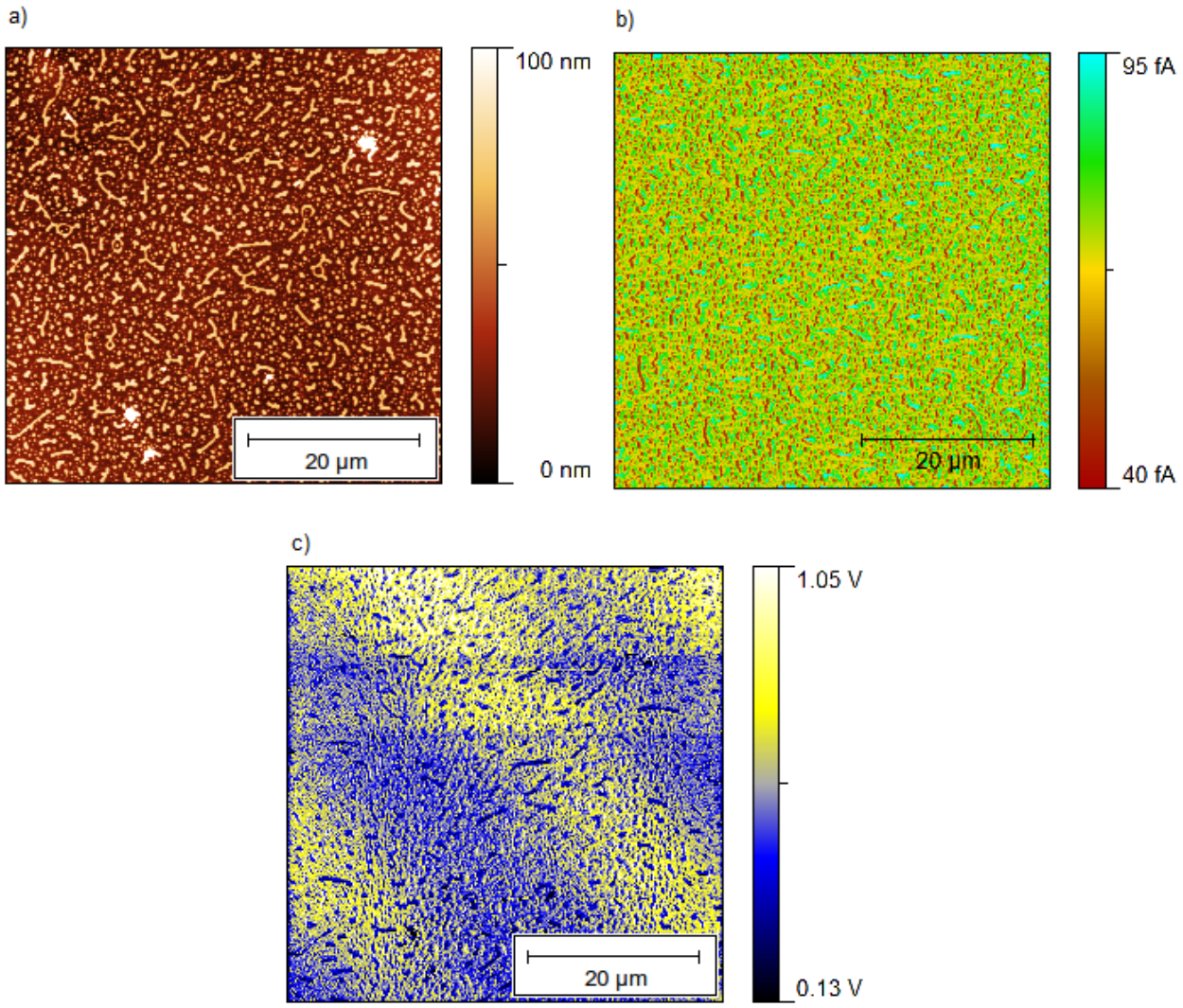

Fig. 21: PPNB/PVK on Si, a) height image, b) current image @ - 8 V, c) friction force image

4.3 PFOT

The Polyformyl-ortho-toluidine (PFOT) films on Au/glass substrates were spin coated and illuminated through a 15 µm lines and spaces mask with UV light by the group of Thomas Griesser at the Institute of Chemistry of Polymeric Materials, University of Leoben. Fig. 22 shows the topography (a) and the current image (b) of PFOT on Au/glass. The different width of illuminated and non-illuminated areas is caused either by a mask with not exactly 15µm lines and spaces or by a half shade of the mask. In the height image, a globular phase and a matrix phase can be distinguished. The RMS roughness is about 13 nm. The globular phase is protruded with structure sizes between 1 µm and 3 µm. This phase

decreases in height under UV illumination. The current image shows stripes containing these particles only in the non-illuminated areas. The matrix exhibits insulating behavior everywhere. Lines from conductive to non-conductive areas are an imaging artifact caused by a too high scan speed. The illuminated, non-conductive areas seem to be homogeneous and are also smoother in the height image. PFOT is decomposing into a conductive and a non-conductive phase. The effect of conductivity is destroyed by UV radiation.

a) b)

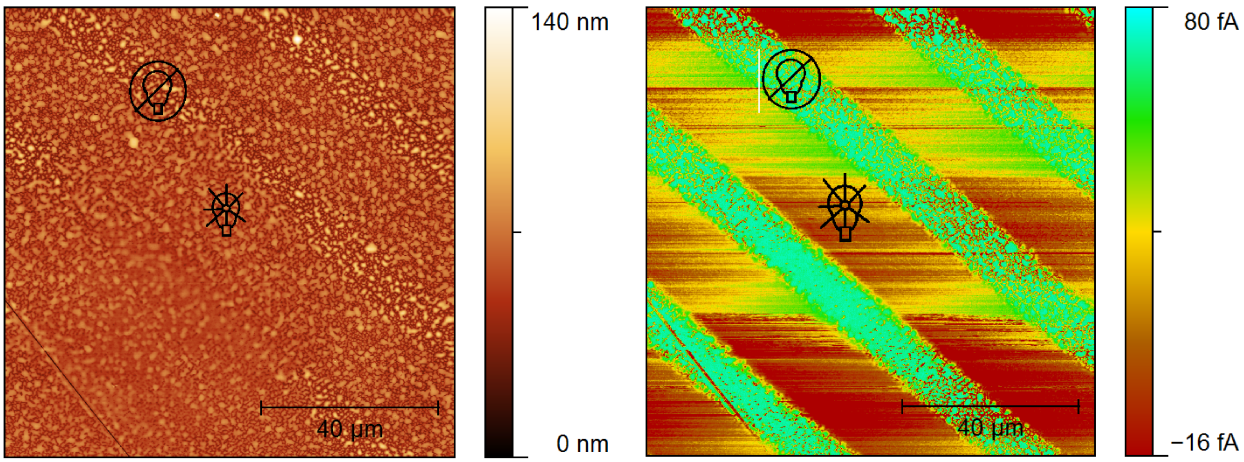

Fig. 22: PFOT on Au/glass, a) height image, b) current image @ + 5 V

4.4 PANI

All Polyaniline (PANI) samples were spin coated on Au/glass and ITO by Simone Radl from the group of Thomas Griesser at the Institute of Chemistry of Polymeric Materials, University of Leoben. The samples were illuminated through a contact mask and - in order to improve the conductivity of the illuminated areas - protonated in HCl vapor.

4.4.1 PANI on Au/glass

Gold together with chromium as an interlayer on glass forms highly conductive and smooth films. Fig. 23 shows the topography (a) and the current image (b), c) and (d) are the corresponding cross sections, of PANI on Au/glass illuminated through a sunlike mask with transparent center. The height image exhibits a rough surface with height differences up to 80 nm and a resulting RMS roughness of 11.8 nm on a 50µm x 50µm scan. There is no influence of illumination on the surface morphology visible. The ripples on the surface might be caused by the substrate or the spin coating and were not further investigated. In the current image, as well as in the profile c) a change in conductivity after illumination and protonation is clearly detected. For an applied voltage of -8 V, the current in the illuminated areas was estimated to be about 50 fA higher than in the non-illuminated areas, as can also be seen in the cross section Fig. 23 c).

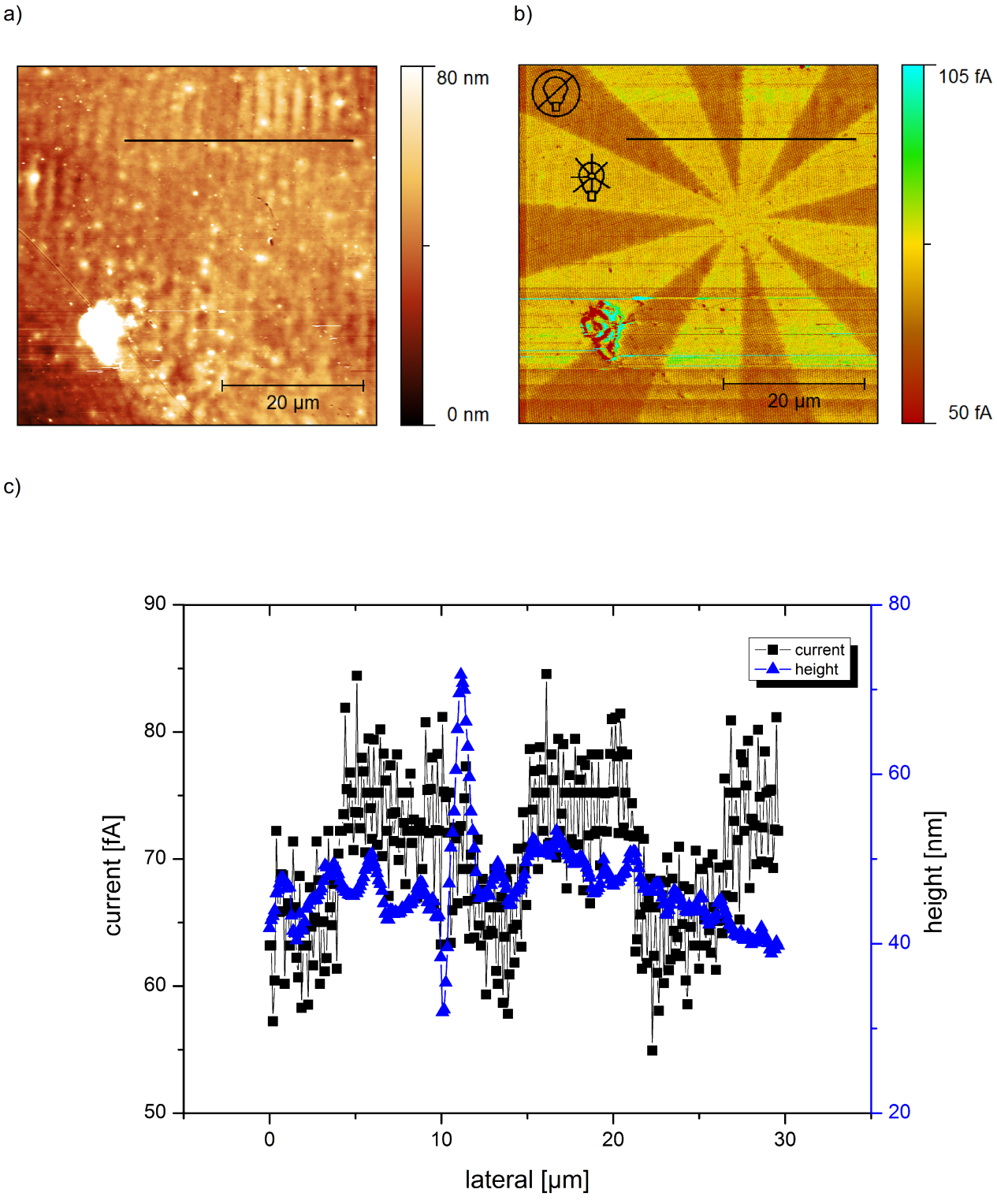

Fig. 23: C - AFM results of PANI on Au/glass after illumination through a proximity mask, a) height image, b) current image @ - 8 V, c) cross section taken along the lines indicated in height and current image

4.4.2 PANI on ITO

ITO is an electrically conductive and optically transparent material, and it is widely used as an electrode in optical devices like displays. These properties and the smooth surface of ITO on glass made us choose it as a substrate material.

Two samples were illuminated through the sunlike mask for different times. After the first investigation the samples were protonated and again analyzed to see the effect of protonation on the illuminated areas. To test the stability of the film and the protonation effect both samples were illuminated again for 55 min without a mask and probed again.

4.4.3 Sample 1; 55 min UV-radiation

Sample 1 of PANI on ITO was illuminated with UV light for 55 min through a mask. An effect of exposure to UV radiation can be seen in the height images [Fig. 24 a), Fig. 25 a), Fig. 26 a)] whereas the illuminated areas are about 10 nm lowered. The exposure to HCl vapor has a disadvantageous influence on the height imaging, which may be caused by a liquid film on the surface as can be seen in Fig. 25 a) and Fig. 26 a). Also a kind of trench between illuminated and non-illuminated areas can be seen in these two height images. The origin of this trench requires further investigation. The RMS roughness increases from 2.3 nm to 3.4 nm during illumination and is not significantly changed after the second illumination. In Fig. 24 b) a change in conductivity can already be seen after illumination, before protonation. But the shift in conductivity of the illuminated areas by about 20 fA is at the noise level of the C-AFM in use, so the positive value of the current is not reliable. After protonation [Fig. 25 b)], the current, at an applied bias of +10 V , on illuminated areas is increased to about -100 pA with an RMS value of 0.67 pA in conductive areas and 8.97 pA in non-conductive areas. The non-illuminated areas are not influenced by protonation in their conductivity. Fig. 25 c) represents a cross section through conductive and non conductive areas in Fig. 25 a) and b). The sharp edge between the conductive and non-conductive areas and the very constant current flow are clearly visible. To test the stability of the effect in conductivity, the samples were illuminated a second time with UV-light for 55 min without a mask. This second UV-illumination [Fig. 26] seems to have a destructive influence on the already illuminated areas. The formerly non-conductive areas

start to become conductive. This can be explained by a self-protonation of the sample. But conductive and non-conductive domains can still clearly be distinguished.

a)

b)

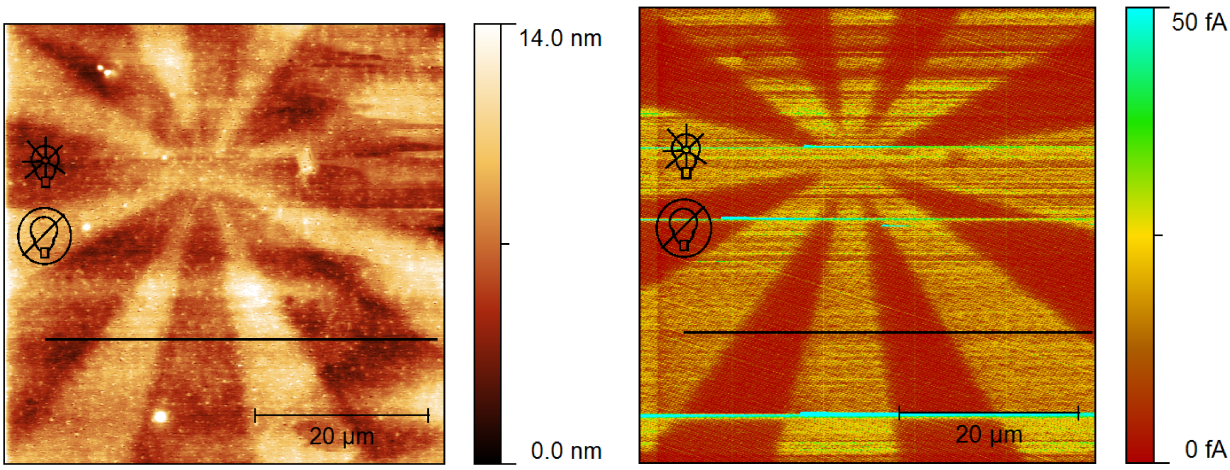

c)

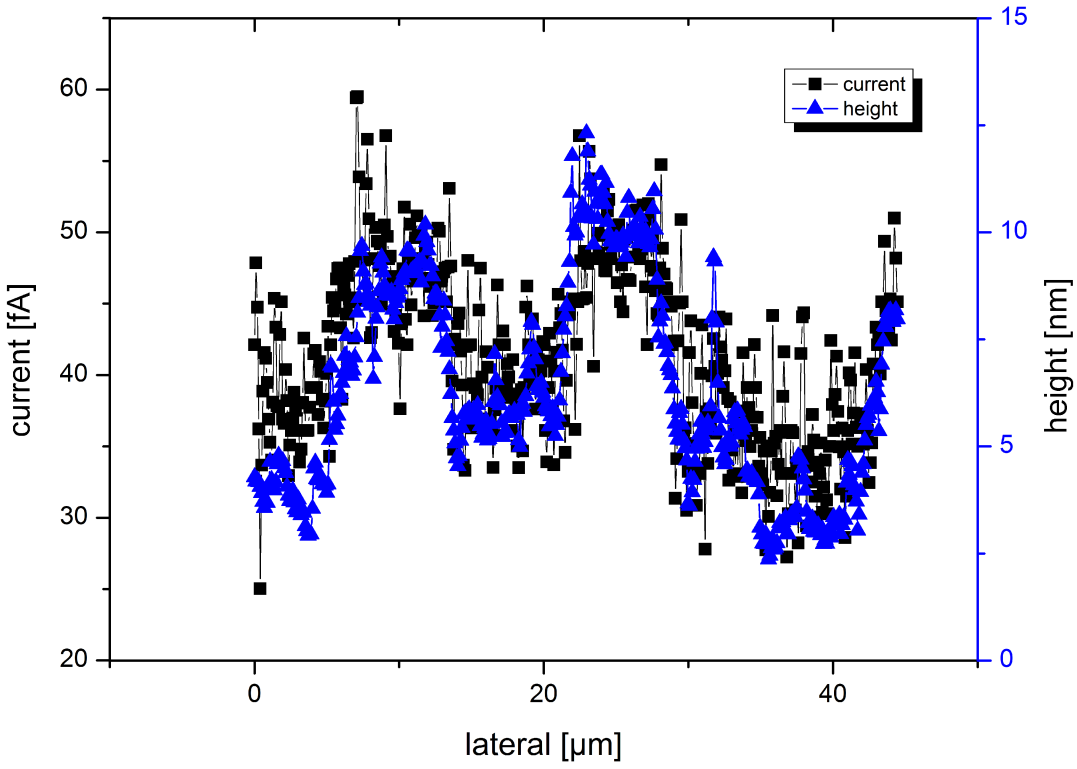

Fig. 24: PANI on ITO, Sample 1, before protonation, a) height image, b) current image @ + 10 V, c) line profile in height and current image

a)

b)

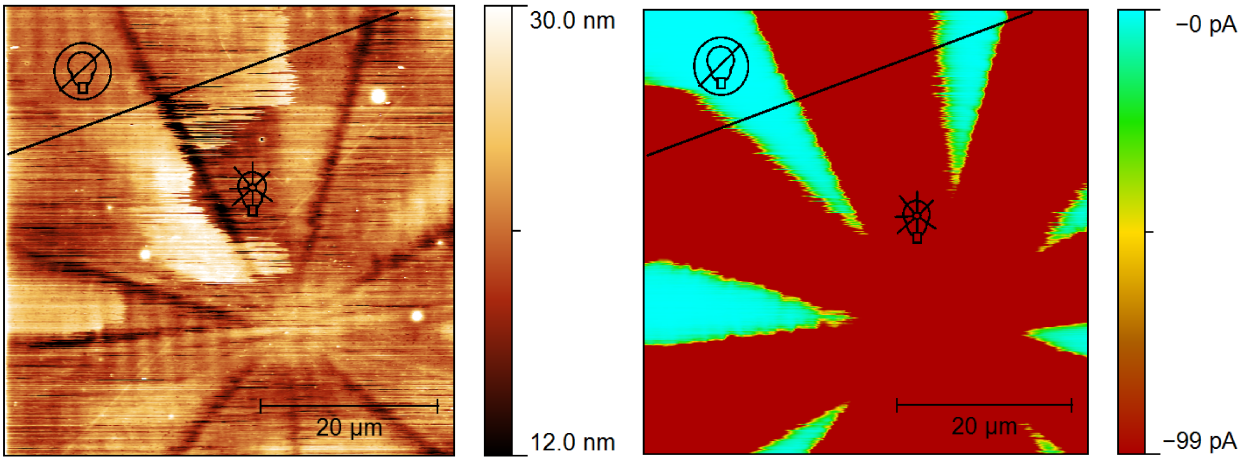

c)

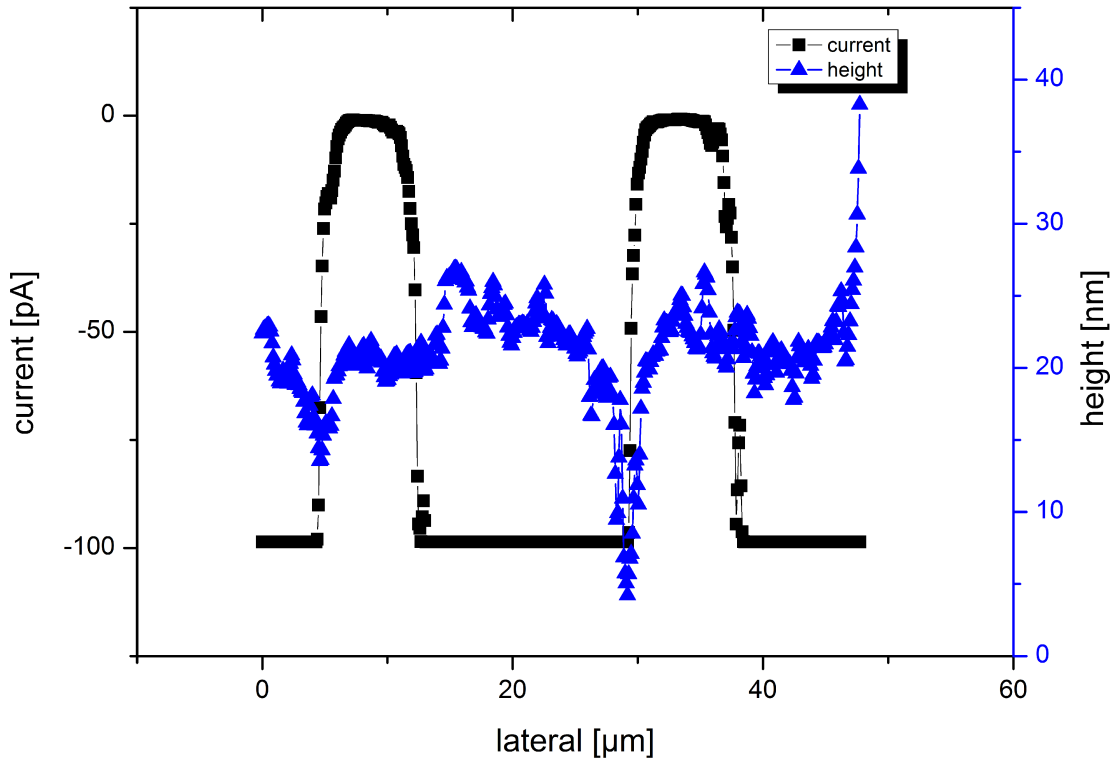

Fig. 25: PANI on ITO, Sample 1, after protonation, a) height image, b) current image @ + 10 V, c) line profile in height and current image

a)

b)

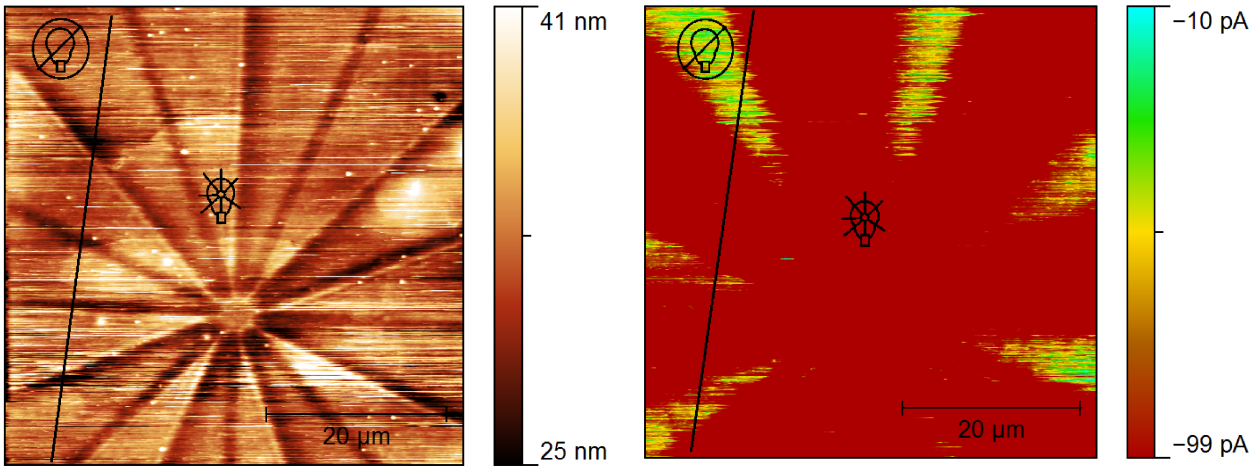

c)

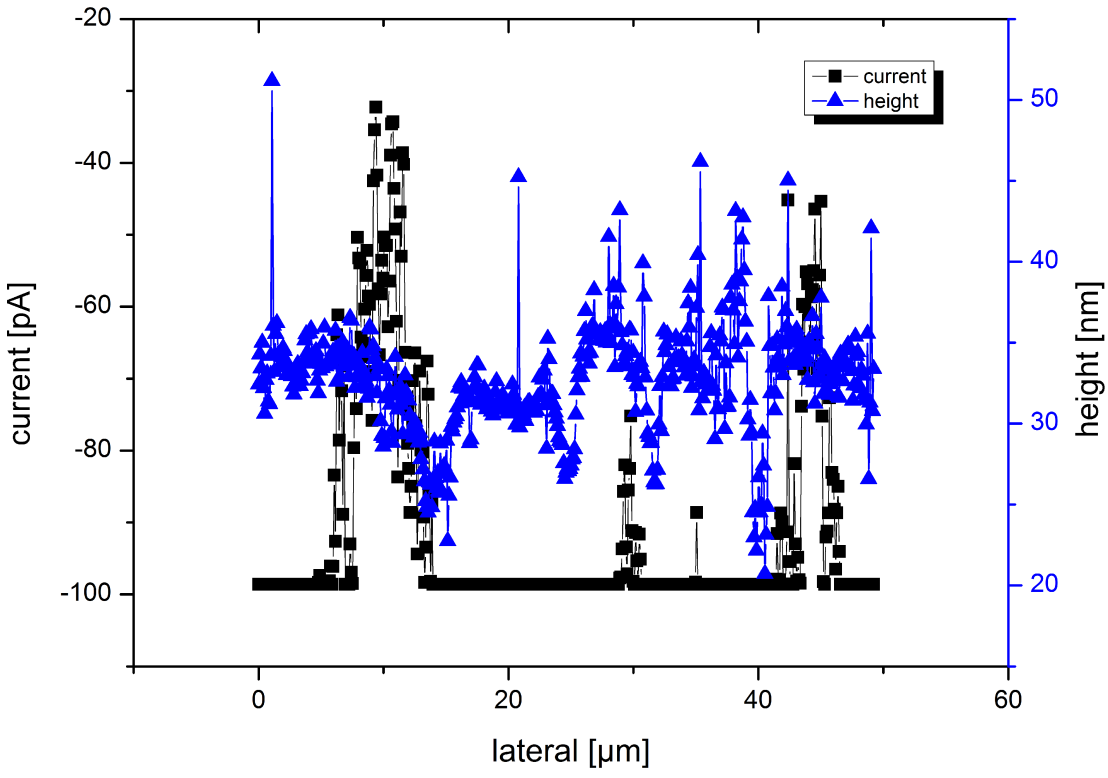

Fig. 26: PANI on ITO, Sample 1, after 2nd illumination, a) height image, b) current image @ + 10 V, c) line profile in height and current image

4.4.4 Sample 2; 25 min UV-Radiation

Sample 2 of PANI on ITO was illuminated for 25 min with UV-light through the same mask as used for sample 1.

In Fig. 27, the height image, the current map and a cross section of the sample after illumination are presented. In the height image a change caused by UV-radiation is clearly visible. Furthermore, elongated particles with a length of about 400 nm are observed. In the current image a change in conductivity of the illuminated areas can clearly be seen. The particle conductivity does not seem to be changed. These particles seem to change their shape after protonation and second illumination, as can be seen in Fig. 28 and Fig. 29. The RMS roughness changes from 3.1 nm to 2.6 nm after protonation and is 5.6 nm after second illumination. After protonation [Fig. 28], the current, at an applied bias of +10 V, is increased on illuminated areas to about -3 pA. The non-illuminated areas are not influenced in their conductivity by protonation. Trenches like those observed for Sample 1 can also be seen. Fig. 29 was mapped after a second UV-illumination for 50 min. The second illumination seems to slightly improve the conductivity of the illuminated areas and has no effect on the non-illuminated zones.

a)

b)

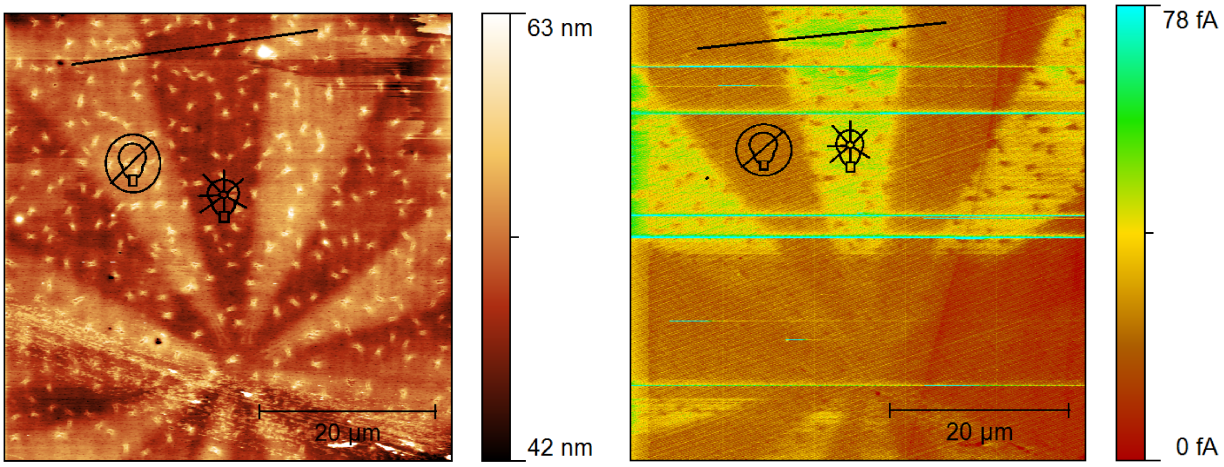

c)

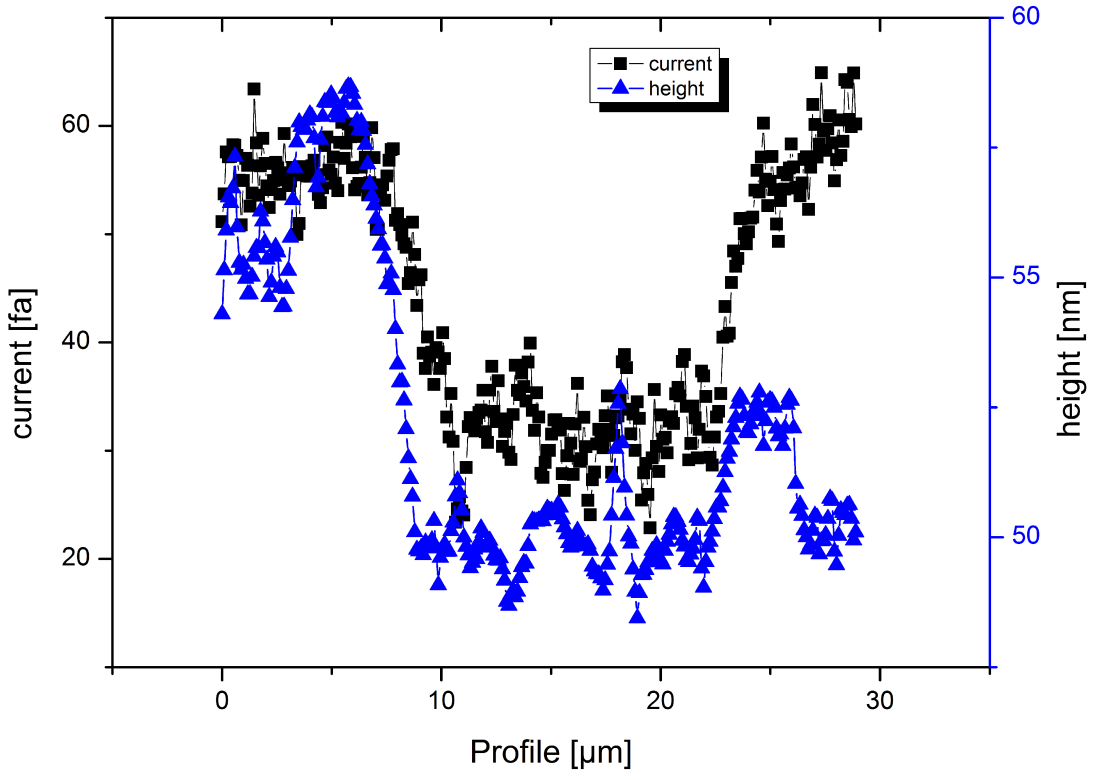

Fig. 27: PANI on ITO, Sample 2, before protonation, a) height image, b) current image @ + 10 V, c) line profile in height and current image

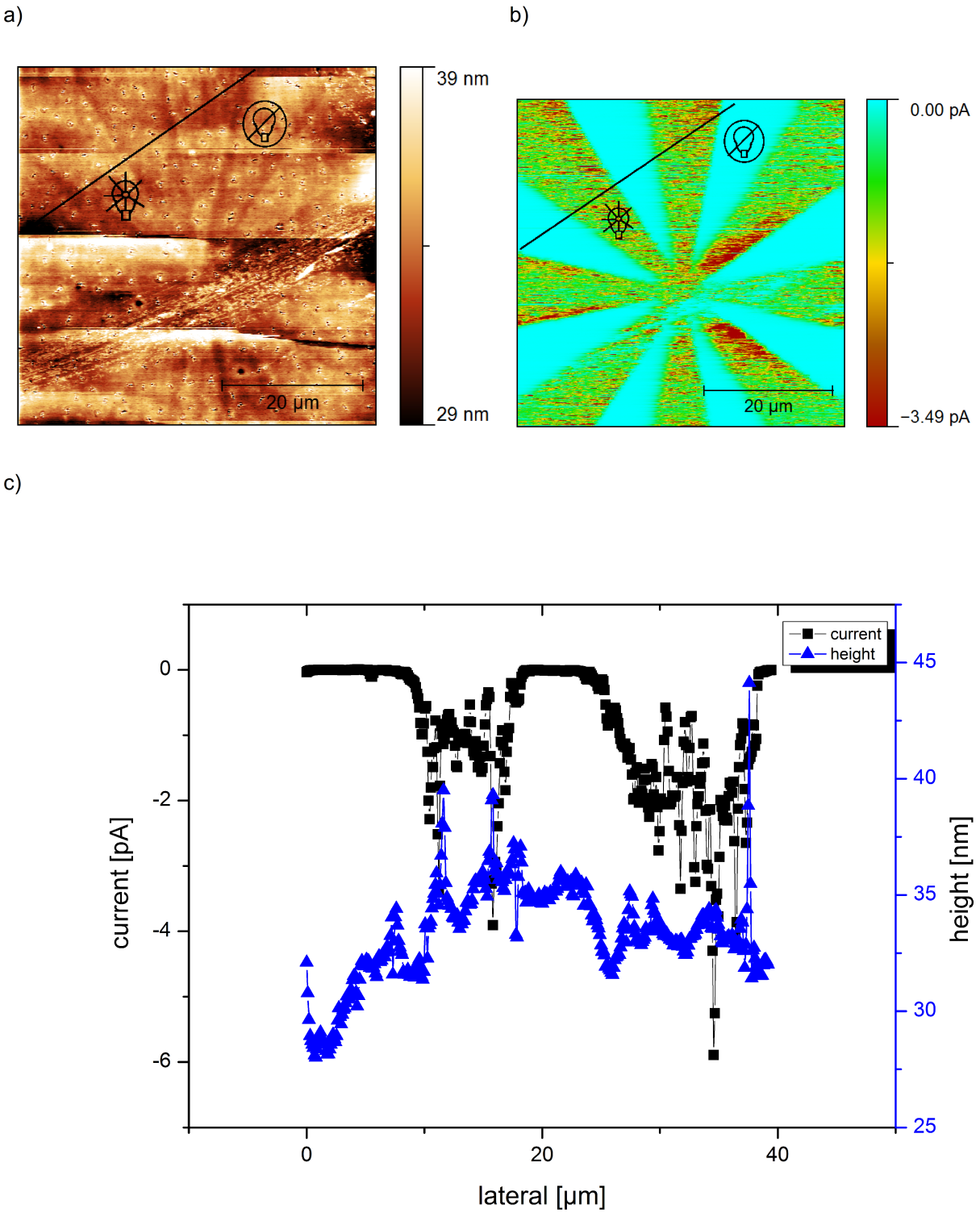

Fig. 28: PANI on ITO, Sample 2, after protonation, a) height image, b) current image @ + 10 V, c) line profile in height and current image

a)

b)

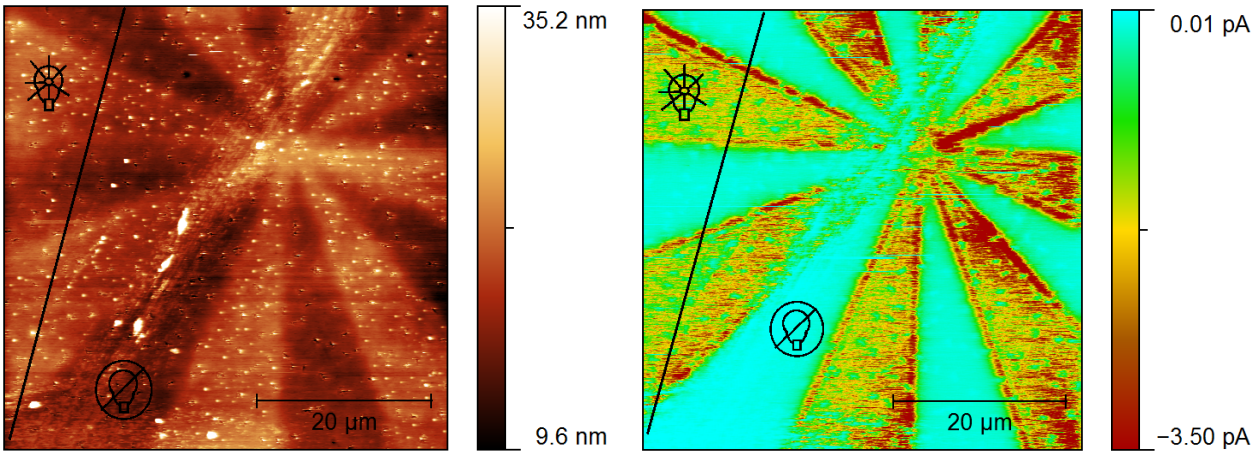

c)

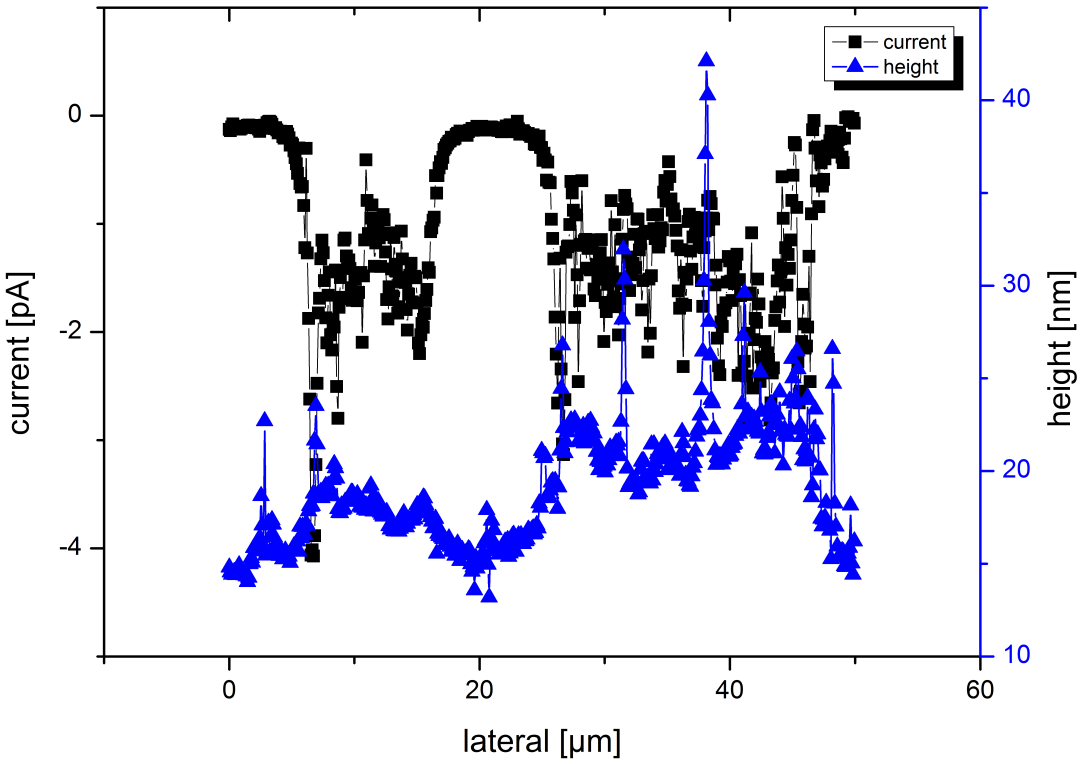

Fig. 29: PANI on ITO, Sample 2, after 2nd illumination, a) height image, b) current image @ + 10 V, c) line profile in height and current image

4.4.5 Comparison of Sample 1 and 2

For both samples a change in topography and electric conductivity after UV-illumination can be measured. In Fig. 30 the values of RMS roughness for both samples are plotted. The change in roughness of sample 2 is significant, whereas sample 1 shows no change in roughness during the treatments. Before protonation the current and height images of the two samples look quite the same. After protonation, the change in conductivity of the 55 min illuminated sample 1 is stronger than in sample 2, which means an incomplete chemical reaction after 25 min illumination. After second illumination both samples keep their behavior in conductivity, and sample two seems to be less damaged than sample 1. However sample 2 is covered by some particles which have probably been modified by illumination.

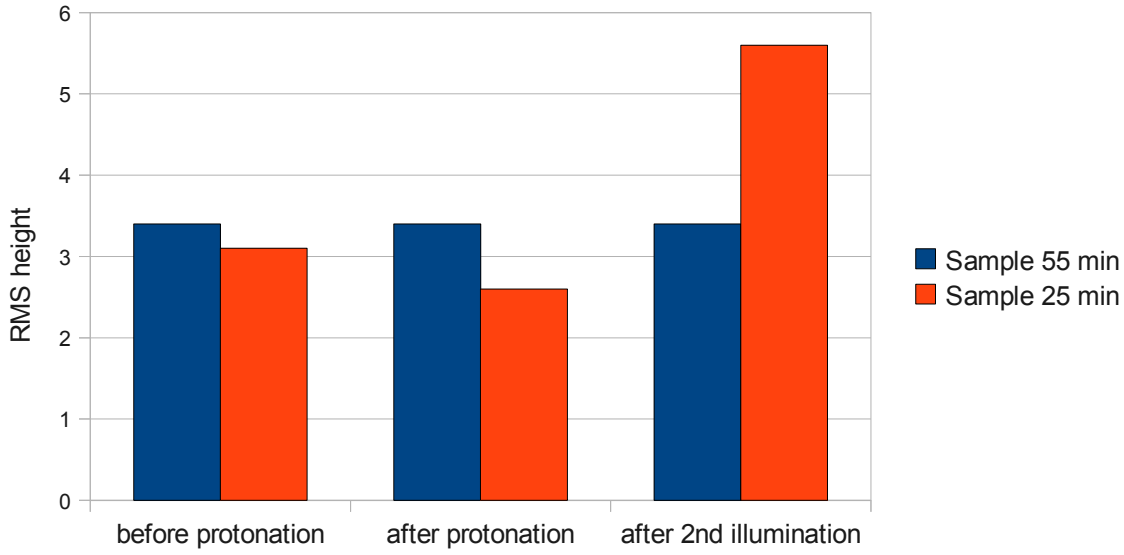

Fig. 30: Comparison of sample 1 and 2 by RMS

5 Conclusions and Outlook

In this thesis, it has been demonstrated that C-AFM is a suitable technique to investigate the morphology and the electric properties of organic thin films. Two systems have been investigated, organic dielectrics and UV-induced photo-reactive, conductive films. In both cases, it was possible to map current images with nanometer resolution.

Parylene samples with various film thicknesses on silicon and Ag/glass substrates were investigated. Problems in parylene mapping were caused by the mechanical properties of the organic film. Parylene tends to stick on the TiN coated C-AFM tips, which makes a current measurement and a topography mapping after a few scan lines impossible. The diamond coated tips scratched the surface. The measurement of I – V curves also destroyed the films locally, and it was not possible to acquire reproducible curves on one spot. Nevertheless, parylene proved a dielectric behavior. The I – V curves on parylene covered areas showed typical Fowler – Nordheim tunneling, whereas ohmic behavior could be seen on the silver substrate. Unfortunately it was not possible to map parylene films on silicon wafers.

In order to find a polymer whose conductivity can be changed, samples of a poly(diphenyl bicyclo[2.2.1]hept-5-ene-2,3-dicarboxylate) (PPNB)/ Poly (N-vinylcarbazole) (PVK) polymer blend, Polyformyl-ortho-toluidine (PFOT) and polyaniline (PANI) were investigated. All these samples were prepared by spin coating and were illuminated with UV-light through a mask. The PPNB/PVK blend did not change the conductivity after UV illumination, but a change in the friction coefficient on the illuminated areas proved a change in chemistry there. PFOT is a conductive polymer, and the illumination changed its conductivity, but the effect was only caused by the destruction of the polymer due to the UV-radiation. PANI is an initially non- conductive polymer which can be made more conductive by UV illumination. The conductivity of the illuminated areas can be further increased by proton doping. It was possible to map those included conductive areas in a non-conductive matrix with high contrast and lateral resolution with C – AFM. This possibility of modification makes PANI a promising candidate for further application as conductive and insulating material in one layer.

Further investigations by C – AFM on organic thin films will be done. Moreover, photoconductive AFM, which is now available in our laboratory, allows to investigate the conductivity in dependence of the wavelength of illuminating light. This can be used to investigate the band structures and the transport mechanisms of polymers. Also in situ measurement of change of conductivity during illumination could be possible. Another new approach is to oscillate the cantilever in torsional direction and to use the change of oscillation frequency as a feedback. In this mode, one could use cantilevers with softer coatings like Pt/Ir and very low contact forces to avoid damage of tip and surface.

6 Appendix

6.1 References

[1] W. Brütting, *Physics of Organic Semiconductors*, Wiley – VCH, Weinheim (2005)

[2] O. G. Reid, K. Munechika, D. S. Gringer Space Charge Limited Current Measurements on Conjugated Polymer Films using Conductive Atomic Force Microscopy, *Nano Lett.*, **6**, 1602 (2008)

[3] L. S. C. Pingree, O. G. Reid, D. S. Ginger, Electrical Scanning Probe Microscopy on Active Organic Devices, A*dvMat* **21**, 19 (2009)

[4] G. Binning, C.F. Quate, Ch. Gerber, Atomic Force Microscope, *Phys. Rev. Lett.* **56**, 930–933 (1986)

[5] G. Meyer, N. M. Amer, Simultaneous measurement of lateral and normal forces with an optical-beam-deflection atomic force microscope, *Appl. Phys. Lett.*, **57**, 2089-2091 (1990)

[6] S. Kremmer, *Dissertation,* Leoben (2005)

[7] D. Sarid, *Exploring scanning probe microscopy with MATHEMATICA*, Wiley – VCH Weinheim (2007)

[8] S. Kremmer, C. Teichert, E. Pischler, H. Gold, F. Kuchar, M. Schatzmayr, Characterization of silicon gate oxides by conducting force microscopy, *Surf. Interface Anal*., **33**, 168 - 172 (2002)

[9] G.P. Petersson, C. M. Svensson, J. Maserjian, Resonance effects observed at the onset of fowler nordheim tunneling in thin MOS structures, *Solid-State Electronics*, **18**, (119 – 451) 1975

[10] Günther Schwabegger, *Diploma Thesis* ,Linz 2009

[11] Y. Shen, A. R. Hosseini, M. H. Wong, G. G. Malliaras, ChemPhysChem, **5**, 16 – 25, 2004

[12] M. Schwoerer, H. C. Wolf, *Organische Molekulare Festkörper*, Wiley - VCH, 2005

[13] http://www.comelec.ch/en/comelec_parylene_specialist.html

[14] R. Hey, Kohärente und inkohärente Streuung elektronischer Zustände in ungeordneten eindimensionalen Systemen, *PhD Thesis*

[15] Griesser, Thomas, T. Höfler, S. Temmel, W. Kern, G. Trimmel *Chem. Mater,* **19**, 3011-3017, (2007)

[16] G. Venugopal, X. Quan, G. E. Johnson, F. M. Houlihan, E. Chin, O. Nalamasu, Photoinduced Doping and Photolithography of Methy – Substitute Polyaniline, *Chem. Mater,* **7**, 271-276, (1995)

[17] D. M. Pai, Transient Photoconductivity in Poly(N-vinylcarbazole), *J. Chem. Phys.* **52**, 2285-2291, (1970)

[18] N. Hanai, M. Sumitomo, Hisao Yanagi, Vapor-deposited poly(N-vinylcarbazole) films for hole transport layer in organic dielectric devices, *Thin Solid Films*, **331**, 106-112, (1998)

[19] S. Radl, *Diploma Thesis*, Leoben, 2010

[20] www.ntmdt.ru

[21] Petr Klapatek, David Necas, Christopher Anderson, Gwyddion user guide

Images

6.2 List of Abbreviations

AFM	Atomic Force Microscopy
C-AFM	Conductive Atomic Force Microscopy
FFM	Friction Force Microscopy
ITO	Indium Tin Oxide
PANI	Polyaniline
RMS	Root Mean Squared
PFOT	Polyformyl-ortho-toluidine
PPNB	Poly(endo,exo-bicyclo[2.2.1]hept-5-ene-2,3-dicarboxylic acid, diphenyl ester) (PPNB)
PVK	Polyvinylkarbazol
PBDV	Pseudo break down voltage

6.3 Acknowledgments

My special thanks go to:

Prof. Christian Teichert for great support and input.

M sc Igor Beinik for the introduction to C – AFM measurements and assistance on many occasions.

Dr. Markus Kratzer and the rest of the Institute of Physics for great support.

Dr. Thomas Griesser for provision with various samples and support.

Bak. Simone Radl from the group of **Prof. Wolfgang Kern** for the preparation of PANI samples.

Günther Schwabegger from the group of **Prof. Helmut Sitter**, JKU Linz, for the providing with parylene samples.

Martin Weiß for the final correction.

the **FWF – NFN** “Interface controlled and functionalized organic thin films” Project S9707-N20 for funding.